Tangent Modulus Method - An Original Method to Measure In-Situ Rock Stress

Fujii, Y.[1], Makasi, M.[2], Kodama, J.[1], Fukuda, D.[1], Goto, K.[3], Kumakura S.[3], Kanaoka, M.[4] and Dassanayake, ABN.[5]

[1]Rock Mechanics Laboratory, Hokkaido Univ., N13W8, Sapporo, JAPAN

[2]Glencore Mount Isa Mines, Mount Isa, Queensland, AUSTRALIA

[3]Docon, 1-5-4-1, Chuo, Atsubetsu, Sapporo, JAPAN

[4]Underground Space Department, Civil Engineering Technology Division, Shimizu Corporation, No.16-1, Kyobashi 2-chome, Chuo-ku, Tokyo, 104-8370, JAPAN

[5]Department of Earth Resources Engineering, University of Moratuwa, Moratuwa 10400, Sri Lanka

Corresponding author's E-mail: fujii6299@frontier.hokudai.ac.jp

Abbreviated title: Tangent Modulus Method to Measure Rock Stress

ABSTRACT

This paper proposed Tangent Modulus Method (TMM) which is an improved oriented core method to determine in-situ rock stresses. In this approach, the cylindrical specimens prepared along different directions from thick core samples were uniaxially compressed twice to a given stress level. The stress value of the bending point in the first loading cycle of the stress-tangent modulus curve is considered as the normal component of the in-situ rock stress along the drilled direction of the specimen. Four types of rocks from soft porous tuff and sandstone to hard crystalline granite was investigated to evaluate the potential of this method. The effects of changes in strain rate, temperature, water content, confining and pore pressure, and stresses larger than the preload on the stress value of the bending point were experimentally investigated on preload specimens to investigate their influence on TMM. Comparison of the stress measurement results by TMM and an overcoring method at AK tunnel in Hokkaido,Japan was also performed to validate the TMM.

Keywords: Tangent Modulus Method; in-situ rock stress; strain rate; temperature; confining pressure

1. INTRODUCTION

As shown in extant studies including Fairhust (2003) and Ljunggren et al. (2003), numerous methods for in-situ rock stress measurement have been developed to date. They are divided into in-situ methods, oriented core methods, and other methods. Oriented core methods can be applied to rock cores from great underground depth and are cheaper and less time consuming than other methods. However, various factors affect the results from oriented core methods, and they are recognized as less reliable than in-situ methods (Ljunggren et al., 2003).

In order to increase the reliability of oriented core methods, previous studies, such as Lavrov (2003), examined the impact of various conditions in the Kaiser effect, and this utilizes acoustic emission (AE) due to the initiation and propagation of microcracks. Experiments indicate that the stress level at the beginning of AE occurrence during uniaxial compression on a triaxially preloaded specimen is equal to the preloaded differential stress value minus 0.5–0.7 times the preloaded confining pressure value. This does not entirely preclude any estimation of in-situ stress, and instead presented a serious problem because the lateral stress is not known in advance. Results also indicate that heating of a saturated diorite or liporite specimen up to 80–100 °C completely eliminates the Kaiser effect. It should also be noted that the Kaiser effect requires a significantly expensive AE measurement system and excellent experimental skills.

Specifically, in the present study, the tangent modulus method (TMM) is presented as a potentially better original oriented core method for stress measurement. The TMM does not require either an AE measurement system or excellent experimental skills. The effect of lateral stress on the result was 1/5th of that from the Kaiser effect (see Section 3.5). The reason is potentially because TMM utilizes the irrecoverable closure of voids as opposed to the initiation and propagation of microcracks (see Chapter 2). The effect of a change in the surrounding water temperature is not significant (see Section 3.2) although it is not possible to perform a quantitative comparison with the aforementioned results for the Kaiser effect because there are differences in the tested rock types.

The procedure for stress measurement using TMM is described first. Subsequently, the effects of changes in strain rate, temperature, water content, confining and pore pressures, and short duration loading of higher stresses (simulating the stress concentration at rock sampling) on the TMM are investigated using laboratory tests. Finally, a comparison between results using the TMM and a stress relief method in the AK tunnel, Japan, is discussed.

2. Tangent modulus method

The following procedure was used to determine in-situ rock stress in the study:

(1) Oriented thick rock cores were sampled from a drilling hole.

(2) Cylindrical rock specimens in various directions were prepared by re-drilling the thick rock core from a drilling hole.

(3) The specimens were uniaxially or triaxially compressed twice to a certain stress level.

(4) The stress value of the bending point in the stress-tangent modulus curve in the first loading cycle or the point where the first and the second stress-tangent modulus curves begin to separate (the point is also subsequently termed as the bending point for the purpose of convenience) was considered as the normal component of the in-situ rock stress in the direction of the specimen.

(5) The three-dimensional stress state was calculated from the normal stress components in more than six independent directions.

In order to demonstrate the potential of the tangent modulus method, the following experiments were performed (Fig. 1):

(1) 30 mmϕ × 60 mm long cylindrical rock specimens were compressed to a given preloading stress level, and the stress was maintained for a set time to simulate in-situ rock stress.

(2) The specimens were unloaded and subsequently cyclically compressed to a higher stress level twice after a delay time.

(3) The stress value at the bending point was compared to the preloading stress value.

As an outline, uniaxial preloading at approximately 30% uniaxial compressive strength (UCS) was applied for 1 h at 295 K, and cyclic loading was performed to approximately 50% UCS at a strain rate of 10^{-4} s^{-1} at 295 K unless other conditions were specified. A time delay was not incorporated although removal and re-installment of end-pieces and clip gages from the specimen were undertaken over one to several minutes. This was performed to ensure that stress memory did not arise due to deformation of the boundary between end-pieces and the specimen or from the clip gage and that measured stresses arose solely from the rock specimen itself. It was assumed that rock specimens did not retain any memory of in-situ rock stress because they were sampled several years prior to performing the experiments and experienced changes in water contents during storage, cutting and grinding using water, and oven-drying for 24 h at 353 K. As shown later in Section 3.3, rock specimens lost their stress memory quickly due to changes in the water content.

The results confirmed that the bending point appeared at the preloading stress level in porous rocks, such as Shirahama sandstone (Fig. 2a) and Kimachi sandstone that both date to the Miocene age, and in a Pleistocene Shikotsu welded tuff under dry conditions (Fujii et al., 2003; Fujii et al., 2008). The bending point was discernible although not quite distinctive in a hard and crystalline Inada granite (Fig. 2b; Fujii et al., 2008). The strengths of these rocks are shown in Table 1. Bending points became more indistinct with increases in the delay time due to relaxation. However, bending points were observed at the preloading stress level even after a delay time of 6 weeks when samples were preloaded for 17 h (Fig. 3). A significantly longer delay time was expected for rocks that were subjected to in-situ stress for geologically long periods.

The mechanism of TMM was explained by nearly irrecoverable closures of rock voids such as microcracks and pores. We assume that A in Fig. 4a denotes the in-situ stress condition under which a rock exhibits a few voids that are tabular and sufficiently large such that they are partly closed, and the rock is stiff during the first cyclic loading up to the in-situ stress level (B to C) because practically none of the voids closed. However, the stiffness decreased under further compression (C to D) due to the closure of the partly closed voids and closure of other open voids. Hence, a bending point appeared at C (Fig. 4b). Further closures did not occur in the second loading cycle, thereby resulting in high stiffness throughout the second loading cycle (E to F). The aforementioned mechanism also correlated well with the principle of Deformation Rate Analysis (DRA), (Yamamoto, 2009), which corresponds to another in-situ rock stress measurement method using oriented cores. In the study, TMM was performed by plotting the tangent modulus (Fig. 4b) since DRA was conducted by plotting the strain difference ($\Delta\varepsilon$ in Fig. 4a) relative to the axial stress under cyclic loading because nonlinearity was not very evident for most real rocks.

3. INFLUENCES OF VARIOUS FACTORS

The above results suggest that TMM could be used as an oriented core method in the future. However, as stated by Lavrov (2003), Ljunggren et al. (2003), and Hsieh et al. (2015), there are several factors that can affect the results of stress measurements by oriented core methods. It was necessary to investigate the effects prior to any practical use of TMM or any other oriented core method. Therefore, effects of changes in the strain rate, temperature, water content, confining and pore pressures, and stress concentration at sampling were investigated.

3.1 Strain rates for cyclic loading

A clear effect of the strain rate for cyclic loading between $10^{-6.5}$ s^{-1} and $10^{-2.5}$ s^{-1} (Fig. 5) was not observed. The specimen lost any stress memory over the long experimental time corresponding to several days for the slowest strain rate of 10^{-7} s^{-1}. Hence, the cyclic loading strain rate did not significantly affect the results provided that it was not excessively slow.

3.2 Temperature of water

Rock mass temperature may not be identical to laboratory room temperature. In order to investigate the effect of the difference in temperature, Kimachi sandstone specimens were preloaded in pure water, unloaded, and cooled in pure water at 295 K for 1 h. Cyclic loading was subsequently promptly applied in air at 295 K. Water temperature between 295 K and 353 K for preloading was not significant (Fig. 6) (Makasi and Fujii, 2008).

3.3 Change in water content

Stress memory was lost very easily with changes in the water content of the specimens. For example, specimens that were preloaded in water lost stress memory quickly after they were dried. Similarly, preloaded dry specimens lost stress memory after they were immersed into water. The results suggested that it was necessary to maintain the water content of rock samples to the maximum possible extent until after cyclic loading stress measurements were completed.

3.4 Triaxial cyclic loading for triaxially preloaded specimens

Triaxial cyclic loading for triaxially preloaded specimens was undertaken because it was not possible to apply uniaxial cyclic loading when in-situ rock stress approaches or exceeds the uniaxial compressive strength of the rock. The apparatus for triaxial compression tests was described in Alam et al. (2014). A loading frame was used to apply the axial load. Axial strain was measured by using strain gages. A double ball plunger pump with a relief valve connected to the ultra-compact triaxial cell (Alam et al., 2014) was used to maintain the confining pressure.

The bending point was observed at smaller stress than the triaxial preloading stress when cyclic loading was undertaken under a smaller confining pressure for dry Shirahama Sandstone (Fig. 7). However, a clear bending point was not observed when cyclic loading was undertaken under a larger confining pressure.

Conversely, the preloading stress was precisely estimated for a smaller confining pressure, and the bending point was observed at a smaller stress level when the confining pressure exceeded the preloaded value (Fig. 8) for dry Kimachi Sandstone. The results appear to contradict each other. However, for example, the set including the highest bending point stress under triaxial cyclic loading and the confining pressure value that exhibited the highest bending point stress may be considered as an in-situ rock stress state although the minimum and intermediate stresses were restricted such that they were identical.

Subsequently, a pair of stainless steel attachments was connected to the saturated and jacketed Kimachi sandstone sample to apply pore pressure. Each attachment included a hole for water flow and a pore pressure sensor. A syringe pump was connected to both attachments and used to produce a constant pore pressure, and the specimens were triaxially preloaded under a pore pressure. Cyclic loading was undertaken under various confining and pore pressures.

Under a constant confining pressure, total and differential stress values at the bending point were obtained by triaxial cyclic loading of a triaxial preloaded saturated Kimachi sandstone sample with a pore pressure between 60% and 140% for preloading (Fig. 9a). In contrast, smaller total and differential stress values at the bending point were obtained under a pore pressure of $\leq$ 20% or $\geq$ 180% for preloading. Terzaghi's effective stress was precisely evaluated only for the case in which the same pore pressure was used.

Based on the data shown in Dassanayake et al. (2015), Biot's effective stress coefficient for Kimachi sandstone is given as follows:

$$\alpha = A - BP'_{\mathrm{C}} \tag{1}$$

where P'_{C} denotes the effective confining pressure, and A and B are constants. We rearrange Eq. (1), and Biot's coefficient is calculated from the total confining pressure P_{C} and pore pressure P_{P} as follows:

$$\alpha = \frac{A - BP_{\mathrm{C}}}{1 - BP_{\mathrm{P}}} \tag{2}$$

We substitute the values of A and B for Kimachi sandstone corresponding to 0.984 and 0.014 MPa^{-1}, respectively, into Eq. (2), and the Biot coefficient is calculated as 0.908. This implies that the effective Terzaghi stress was almost identical to the effective Biot stress in this case. Therefore, only the effective Terzaghi stress is shown here.

A smaller total preloading stress was investigated under pore pressure and under a constant effective confining pressure for a cyclic loading smaller than that of the preload (Fig. 9b). The effective and differential preloading stress was measured as lower when pore pressure exceeding that of the preloading was used.

3.5 Uniaxial cyclic loading for triaxially preloaded specimens

Uniaxial cyclic loading was performed for triaxially preloaded saturated Kimachi sandstone under a range of confining and pore pressures. The preloaded differential axial stress corresponded to 12 MPa for all the specimens. The effect of pore pressure was obtained as negligible (Fig. 10). The bending point stress decreased with respect to the confining pressure at preloading. We approximated the results with a linear superposition of axial stress, confining pressure, and pore pressure in preloading to obtain the following expression:

$$\sigma_B = (0.93 \pm 0.07)\sigma - (1.05 \pm 0.11)P_C - (0.002 \pm 0.15)P_P \quad (3)$$

or

$$\sigma_B = (0.93 \pm 0.07)\Delta\sigma - (0.11 \pm 0.11)P_C - (0.002 \pm 0.15)P_P \quad (4)$$

where σ_B, σ, P_C, P_P, and $\Delta\sigma$ denote the bending point stress, preloaded axial total stress, preloaded confining pressure, preloaded pore pressure, and preloaded axial differential stress, respectively. The negligible effect of pore pressure in the test series was obtained by chance. The sensitivity of the bending stress value (0.11 in Eq. (4)) to the preloading confining pressure was approximately 1/5 of that obtained in the Kaiser effect. This demonstrated an advantage of the TMM when compared to the Kaiser effect.

3.6 Effect of stress exceeding preload albeit applied for a shorter duration

The dry Kimachi sandstone specimens were subject to the following:

(1) compression at 30% UCS for 24 h as a preload to simulate in-situ rock stress;
(2) compression up to 40% UCS by a triangular loading pattern for approximately 1 min to simulate the stress concentration at rock sampling (Fig. 11);
(3) unloading and maintaining for specified delay times; and subsequently,
(4) cyclic loading twice up to 50% of UCS to obtain the stress-tangent modulus curves.

All loading and unloading operations were undertaken at a strain rate of 10^{-4} s^{-1}. Seven specimens were tested with delay times corresponding to a maximum of 1 week.

Bending points were observed at 40% UCS (16 MPa) for delay times between 0 and 1 hour (Fig. 12a–c). This indicated that the memory of the long term-preload was erased under higher short term stress. Bending points were observed at 30% UCS (12 MPa) and 40% UCS for a delay time of 3 h (Fig. 12d). This indicates that memories of both the long-term preload and the higher short-term load were detected. Bending points were observed only at 30% UCS after delay times of 1 d and 3 d (Fig. 12e and f). The memory of the larger short-term stress was lost and only the memory of the long-term preload was detected. A bending point was not observed for a delay time of 1 week (Fig. 12g), and thus the memories of both loads were lost.

4. DISCUSSION

The experimental results are summarized as follows:

(1) The bending point appears at the preloading stress level in the axial stress-tangent modulus diagram during cyclic loading for four dry rocks. Bending points are observed under the preloading stress level even after a delay time of 6 weeks after 17 h of preloading.

(2) A clear effect of strain rates for cyclic loading is not observed with the exception of the slowest strain rate at which the specimen lost stress memory during the long experimental duration.

(3) A clear effect of preloading water temperature is not observed between 295 K and 353 K.

(4) Stress memory is lost very easily when the water content of the specimens change. The water content of rock cores should be maintained unchanged to the maximum possible extent until stress measurements by cyclic loading are completed.

(5) Confining pressure during triaxial cyclic loading affects the bending point stress value.

(6) Pore pressure during triaxial cyclic loading affects the bending point stress value.

(7) In uniaxial cyclic loading for triaxially preloaded rocks, confining pressure for preloading affects the bending point stress value although the effects of the pore pressure are negligible.

(8) It is estimated that the memory of a larger stress over a short time at rock sampling is lost, and it is potentially possible to evaluate a precise value of the normal component of in-situ rock stress (which acted over geological time in the direction of the specimen) if an appropriate delay time is set.

Results (1)–(3) and (8) prompt further investigation and improvement of the tangent modulus method. Result (4) may be considered as a practical albeit difficult guideline. Results (5) and (6) are academically interesting although they do not warrant further investigation because it is significantly easier to perform uniaxial cyclic loading than triaxial cyclic loading. Result (7) leads to the conclusion that it is necessary to consider lateral stress components other than axial stress, and the result appears natural because rock deformation is strongly affected by confining pressure. An estimation of the three-dimensional stress state is potentially possible by combining Eq. (3) or Eq. (4) for more than seven directions (or six directions if pore pressure is ignored). It should be noted that this does not mean that more than six holes are required. Specimens in various directions are prepared from a thick rock core from a drill hole. For example, 30-mm thick and 60-mm long specimens in any direction are prepared by re-drilling from a rock core with a diameter exceeding 67.1 mm. However, further investigations should be performed for the cases in which the directions of specimen do not coincide with the principal stress directions. The negligible effect of pore pressure is useful to estimate the normal stress value. Conversely, this limits the estimation of pore pressure by TMM. This does not lead to significant disadvantages because in-situ pore pressure can be measured by other means. However, the negligible effect is potentially obtained by chance and should be investigated further with respect to other rock types.

5. Case study at AK tunnel in Hokkaido, Japan

Stress measurements were performed at AK tunnel in Hokkaido, Japan (Goto et al., 2007 in Japanese and Kawamura et al., 2006 in Japanese) in 2005 by using TMM and the pilot hole wall deformation method. The latter method is a stress relief method utilizing changes in diameter in three directions and axial displacements along four directions during overcoring (Lee et al., 2009). The method does not require a strain gage attachment to the borehole wall and instead measures displacement using mechanical transducers. Therefore, it is expected as suitable for severe conditions such as muddy sludges and rough borehole walls. The Cretaceous and highly fractured rock mass consisted of hard sandstone with a UCS of 237 MPa and a 50% tangent modulus of 55 GPa.

The N62°W horizontal borehole was drilled from the sidewall of the tunnel. The overburden was 98 m and overcoring was attempted at depths corresponding to 1.0, 5.4, 7.4, and 8.4 m. Displacement during overcoring was only recorded at the depth of 8.4 m due to the highly fractured nature of the rock mass. The calculated maximum, intermediate, and minimum principal stresses were 43, 6, and –13 MPa, respectively (Fig. 13). The displacement behavior due to stress relief was considerably unstable, and the calculated stresses could potentially contain errors. However, it is noted that the rock stress significantly exceeded the overburden pressure and was nearly uniaxial.

Stress measurement using TMM was performed on the rock core from the aforementioned drill hole. The 150-mm thick core was highly fractured, and samples at approximately 1 m from the sidewall with relatively fewer fractures were used for the tests. Ideally, specimens in six independent directions are required to obtain the stress tensor. However, 30-mm thick and 60-mm long specimens in the axial direction (V) and the two perpendicular directions (P1 and P2) were prepared by re-drilling the thick rock core because the length of the thick core was insufficient and the thick core was not orientated due to fractures. The rock core was maintained as immersed in tap water, and the test was performed as soon as possible (10 d after the sampling) to minimize the loss of stress memory.

The wet specimens were quickly cyclic loaded in air at 10^{-4} s^{-1} after 10 days of in-situ sampling. Bending points were detected for five out of six V specimens (Fig. 14) and in all three P1 specimens. A bending point was not detected in the four P2 specimens. Average bending point stress corresponded to 30.8±6.0 MPa in V and 25.4±7.7 MPa in P1. It was not possible to directly compare the results with the results discussed above as obtained from the overcoring method. However, bending points were detected for the hard sandstone specimens from in-situ rock mass, and the stress level at the bending point was similar to the maximum principal stress from an overcoring method.

6. CONCLUDING REMARKS

In the study, TMM for measurement of in-situ rock stress was proposed as an improved oriented core method. The procedure to determine in-situ rock stress by TMM was as follows: Oriented rock cores were sampled from the site and cylindrical rock specimens were constructed, and the specimens were uniaxially or triaxially compressed twice to a given stress level. The stress value of the bending point in the stress-tangent modulus curve in the first loading cycle or the point where the first and the second stress-tangent modulus curves begin to separate (the point was also termed as the bending point for convenience) was considered as the normal component of in-situ rock stress in the direction of the specimen.

In order to evaluate the potential of the method, the existence of a bending point for four uniaxially preloaded dry specimens of rock from soft porous tuff and sandstones to a hard crystalline granite was investigated. The effects of the strain rate, changes in temperature or water content, confining and pore pressures, and stresses exceeding the preload on the bending pint stress value were also experimentally investigated on the preloaded specimens. The main results were as follows: (1) The bending point appeared at the preloading stress level in the axial stress-tangent modulus diagram during the cyclic loading for four dry rocks, and the points were observed at the preloading stress level even after a time delay of 6 weeks for 17 h of preloading; (2) a clear effect of the strain rate for the cyclic loading was not observed with the exception of the slowest strain rate at which the specimen lost any stress memory given the long experimental duration; (3) a clear effect of preloading water temperature between 295 K and 353 K was not observed; (4) stress memory was very easily lost when the water content of specimens changed, and thus it was necessary to maintain the water content of rock cores to the maximum possible extent until stress measurement by cyclic loading was completed; (5) the confining pressure during triaxial cyclic loading affected the bending point stress value; (6) the pore pressure during triaxial cyclic loading affected the bending point stress value; (7) in uniaxial cyclic loading for triaxially preloaded rocks, the confining pressure for preloading affected the bending point stress value while the effects of pore pressure were negligible; and (8) the memory of higher stresses over a short time at rock sampling was lost, and it was potentially possible to evaluate the precise value of the normal component of in-situ rock stress (which acts over geologically-long times in the specimen direction) if an appropriate delay time was set.

In the case study at AK tunnel in Hokkaido, Japan, it was confirmed that bending points were detected for rock specimens from in-situ rock mass, and that the stress level at the bending point was similar to the maximum principal stress by using an overcoring method.

It is expected that future studies will focus on investigating the tangent modulus method in detail, improve on the same, and widely used it to measure in-situ rock stress.

REFERENCES

Alam, B., Niioka, M., Fujii, Y., Fukuda, D., Kodama, J., 2014. Effects of confining pressure on the permeability of three rock types under compression. Int. J. Rock Mech. Min. Sci. 65, 49-61.

Dassanayake, A.B.N., Fujii, Y., Fukuda, D., Kodama, J., 2015. A new approach to evaluate effective stress coefficient for strength in Kimachi sandstone. J. Petrol. Sci. Engng. 131, 70-79.

Fairhurst, C., 2003. Stress estimation in rock: A brief history and review. Int. J. Rock Mech. Min. Sci. 40, 957-973.

Fujii, Y., Ohtaka, N., Nakagawa, Y., Kodama, J., 2006 in Japanese. A study on estimation of rock stress based on variation of tangent modulus. J. MMIJ. 122, 483-488.

Fujii, Y., Ohtaka, N., Nakagawa, Y., Kodama, J., 2008 in Japanese. Tangent Modulus Method, applicability to three types of rock and influence of confining pressure. J. MMIJ. 124, 120-128.

Goto K., Kumakura, S., Kawata, T., Fujii, Y., 2007 in Japanese. A case study on stress measurement at a tunnel damaged due to sqeezing of rock mass. *In* Forum 2007 Sapporo, Geotechnical Consultants Association.

Hsieh, A., Dight, P., Dyskin, A.V., 2015. The rock stress memory unrecoverable by the Kaiser effect method. Int. J. Rock Mech. Min. Sci. 75, 190-195, doi:10.1016/j.ijrmms.2015.01.006

Kawamura, S., Shima, Y., Kawata, T., Kanaoka, K., 2006 in Japanese. Breakthrough achieved through a double support structure for a construction involving landslide of an unexpected scale. Tunnels and Underground. 37, 895-903.

Lavrov, A., 2003. The Kaizer effect in rocks: principles and stress estimation techniques. Int. J. Rock Mech. Min. Sci., 40, 151-171.

Lee, K., Ishijima, Y., Fujii, Y., Koo, H. B., 2009. Development of rock stress measurement probe based on the Pilot Hole Wall Deformation Method laboratory tests. *In* Proc. 43rd. U.S. and 4th U.S. Canada Rock Mechanics Symposium, Asheville 2009, ARMA 09-131

Ljunggren, C., Chang, Y., Janson, T., Christiansson, R., 2003. An overview of rock stress measurement methods. Int. J. Rock Mech. Min.Sci. 40, 975-989.

Makasi M., Fujii Y., 2008. Effects of strain rate and temperature on Tangent Modulus Method. *In* Proc. Korean Rock Mechanics Symposium 2008 (KRMS 2008), 279-285, Chonnam National University Gwangju, Korea, Oct. 22

Yamamoto, K., 2009. A theory of rock core-based methods for in-situ stress measurement. Earth Planets and Space, 61, 1143-1161.

Captions of figures

Fig. 1 Preloading and cyclic loading. 1 and 2 mean the first and the second loading cycle, respectively.

Fig. 2 Examples of stress-tangent modulus curve in cyclic loading. 1 and 2 mean the first and the second loading cycle, respectively. Strain rate and preloading duration were 10^{-5} s^{-1} and 60 min. for Shirahama sandstone. They were 10^{-4} s^{-1} and 100 min. for Inada granite.

Fig. 3 Maximum delay time for stress memory with duration of preload application t_L for dry Shirahama Sandstone. Strain was measured by a clip gage.

Fig. 4 Schematic figures showing deformation of a very nonlinear rock.

Fig. 5 Influence of strain rates for the cyclic loading of dry Kimachi sandstone. Strain was either measured by a clip gage or evaluated from stroke.

Fig. 6 Influence of water temperature for preloading of Kimachi sandstone

Fig. 7 Influence of confining pressure change at cyclic loading for dry Shirahama sandstone. Confining pressure and axial stress for preloading was 5 MPa and 15.8 MPa, respectively.

Fig. 8 Influence of confining pressure change at cyclic loading for dry Kimachi sandstone. Confining pressure and axial stress for preloading is 10 MPa and 29 MPa, respectively.

Fig. 9 Influence of pore pressure on bending point stress for saturated Kimachi sandstone. Total confining pressure, pore pressure and total axial stress for preload were 10 MPa, 5 MPa and 22 MPa, respectively.

Fig. 10 Bending point stress by uniaxial cyclic loading for triaxially preloaded saturated Kimachi Sandstone. Preloaded differential axial stress was 12 MPa for all specimens. Preloaded pore pressure was 5 MPa except for 0.9 MPa and 4.9 MPa for confining pressure of 1 MPa and 5 MPa, respectively in (b). Strain was based on a clip gage.

Fig. 11 Preloading, larger stress application for short period and cyclic loading.

Fig. 12 Stress-tangent modulus curves. Pre-stress and short time-larger stress are 12 MPa and 16 MPa, respectively. Strain was measured by the clip gage. Red and blue curves show the first and the second loading, respectively.

Fig. 13 Stereo projection of the stress state (MPa) measured using the pilot hole wall displacement method at AK tunnel onto the lower hemisphere.

Fig. 14 An example of stress-tangent modulus curve pairs for specimen V-1.

Figures

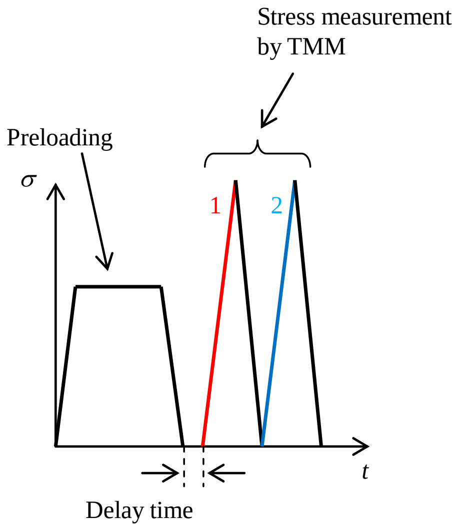

Fig. 1 Preloading and cyclic loading. 1 and 2 mean the first and the second loading cycle, respectively.

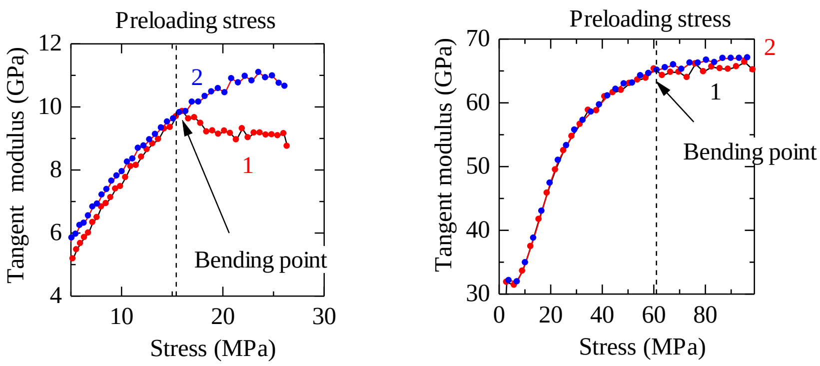

(a) Dry Shirahama sandstone (b) Dry Inada granite

Fig. 2 Examples of stress-tangent modulus curve in cyclic loading. 1 and 2 mean the first and the second loading cycle, respectively. Strain rate and preloading duration were 10^{-5} s^{-1} and 60 min. for Shirahama sandstone. They were 10^{-4} s^{-1} and 100 min. for Inada granite.

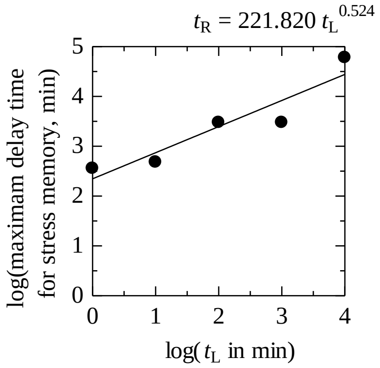

Fig. 3 Maximum delay time for stress memory with duration of preload application t_L for dry Shirahama Sandstone. Strain was measured by a clip gage.

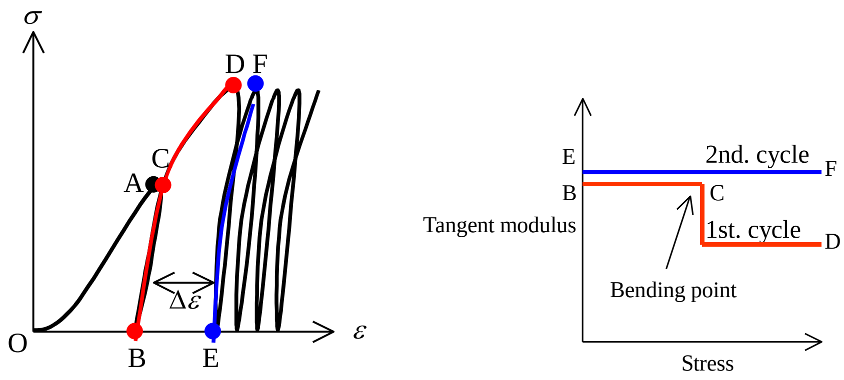

(a) Stress-strain curve (b) Stress-tangent modulus curve

Fig. 4 Schematic figures showing deformation of a very nonlinear rock.

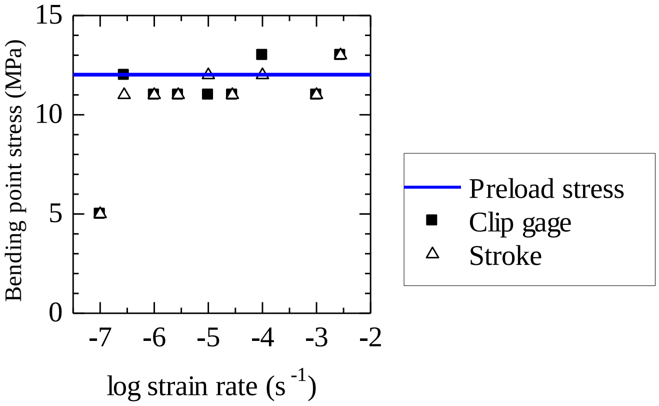

(a) Influence of strain rate

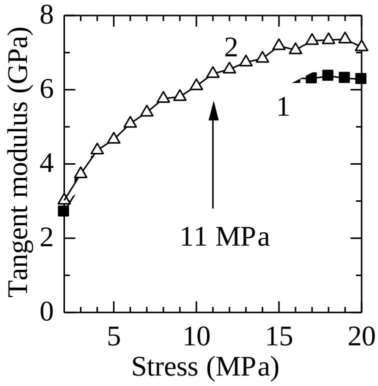

(b) 10^{-3} s^{-1} (stroke base)

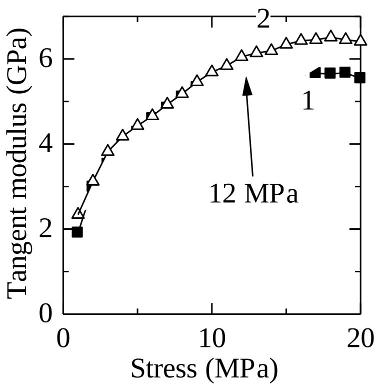

(c) 10^{-6} s^{-1} (stroke base)

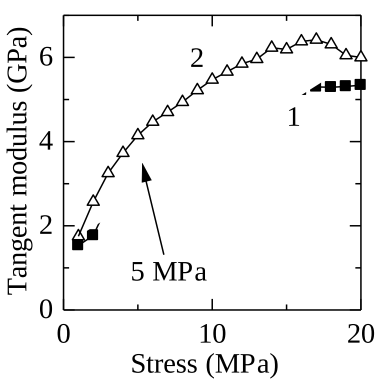

(d) 10^{-7} s^{-1} (stroke base)

Fig. 5 Influence of strain rates for the cyclic loading of dry Kimachi sandstone and examples of stress-tangent modulus curves. Strain was either measured by a clip gage or evaluated from stroke.

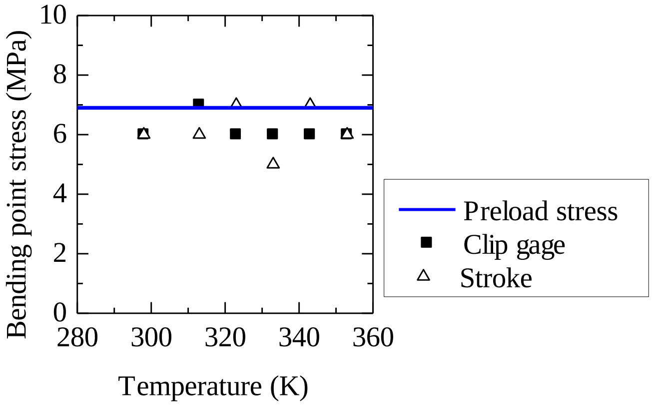

Fig. 6 Influence of water temperature for preloading of Kimachi sandstone

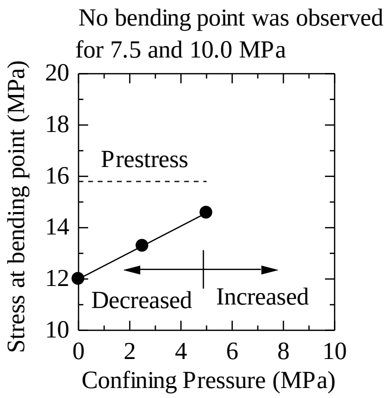

Fig. 7 Influence of confining pressure change at cyclic loading for dry Shirahama sandstone. Confining pressure and axial stress for preloading was 5 MPa and 15.8 MPa, respectively.

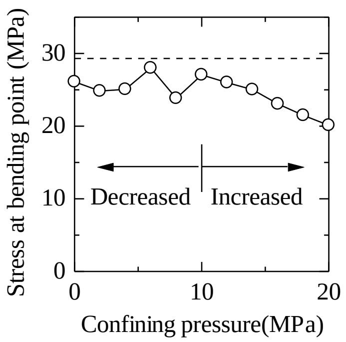

Fig. 8 Influence of confining pressure change at cyclic loading for dry Kimachi sandstone. Confining pressure and axial stress for preloading is 10 MPa and 29 MPa, respectively.

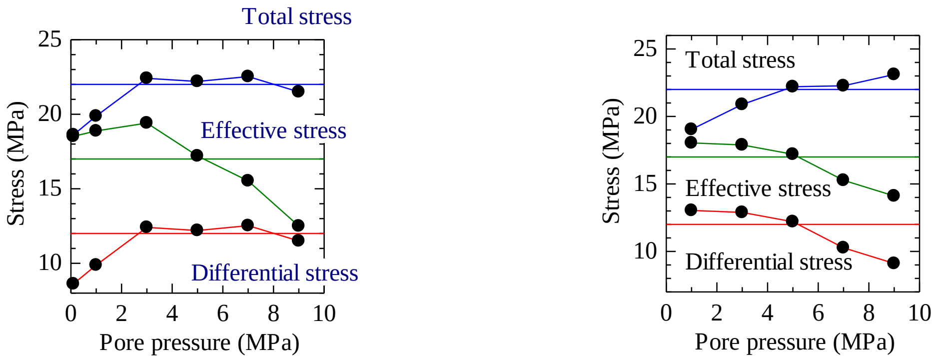

(a) Constant total confining pressure of 10 MPa (b) Constant effective confining pressure of 5 MPa

Fig. 9 Influence of pore pressure on bending point stress for saturated Kimachi sandstone. Total confining pressure, pore pressure and total axial stress for preload were 10 MPa, 5 MPa and 22 MPa, respectively.

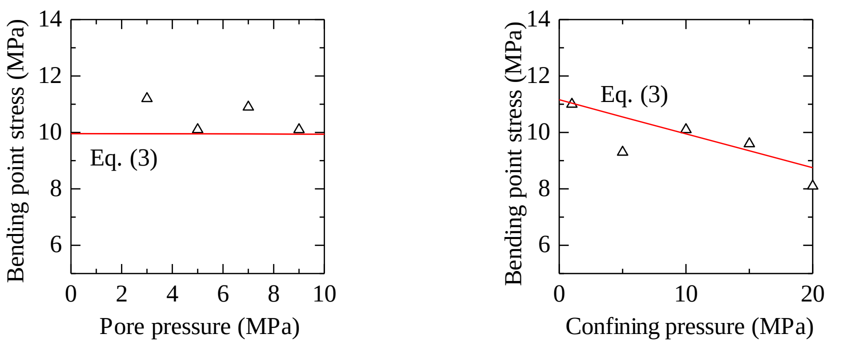

(a) Constant confining pressure of 10 MPa (b) Nearly constant pore pressure of 5 MPa

Fig. 10 Bending point stress by uniaxial cyclic loading for triaxially preloaded saturated Kimachi Sandstone. Preloaded differential axial stress was 12 MPa for all specimens. Preloaded pore pressure was 5 MPa except for 0.9 MPa and 4.9 MPa for confining pressure of 1 MPa and 5 MPa, respectively in (b). Strain was based on a clip gage.

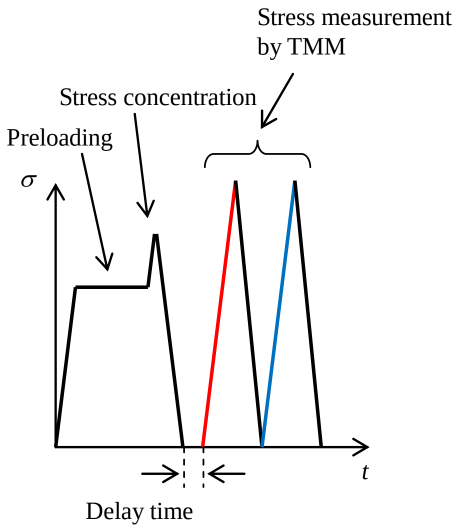

Fig. 11 Preloading, larger stress application for short period and cyclic loading.

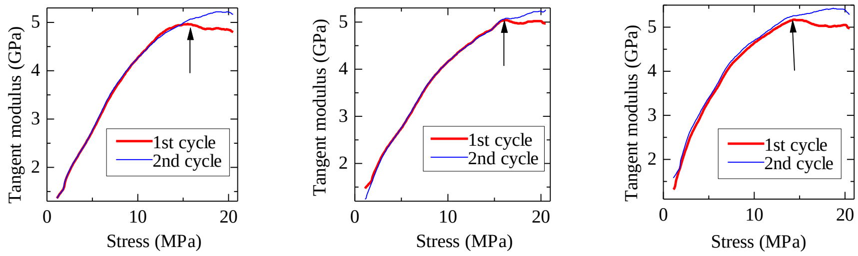

(a) No delay time (c) 30 min. delay (d) 1 hour delay

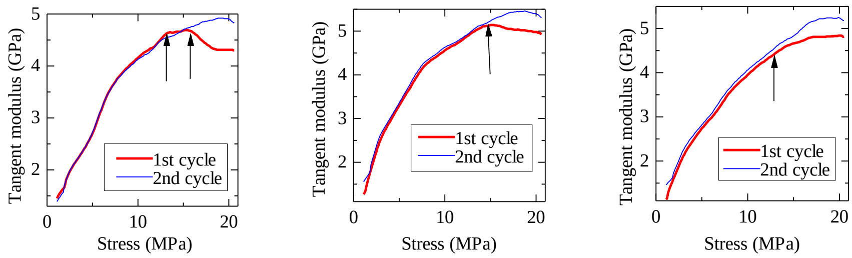

(e) 3 hour delay (f) 1 day delay (g) 3 day delay

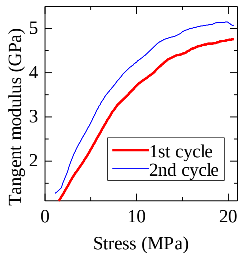

(h) 1 week delay

Fig. 12 Stress-tangent modulus curves. Pre-stress and short time-larger stress are 12 MPa and 16 MPa, respectively. Strain was measured by the clip gage. Red and blue curves show the first and the second loading, respectively.

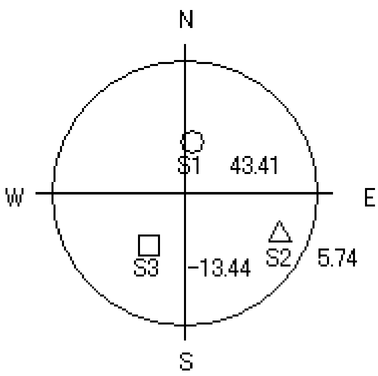

Fig. 13 Stereo projection of the stress state (MPa) measured using the pilot hole wall displacement method at AK tunnel onto the lower hemisphere.

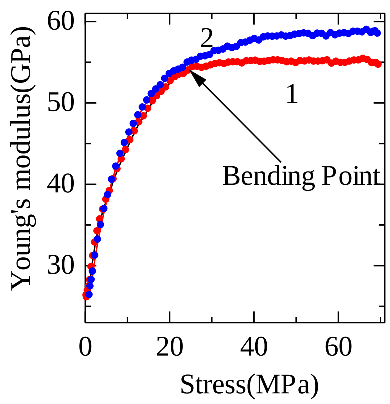

]

Fig. 14 An example of stress-tangent modulus curve pairs for specimen V-1.